Fire Technology, 54, 1249–1263, 2018

Manufactured in The United States
https://doi.org/10.1007/s10694-018-0727-x

Fire Detection Algorithm Combined with Image Processing and Flame Emission Spectroscopy

Xuanbing Qiu, Tingyu Xi, Dongyuan Sun, Enhua Zhang, Chuanliang Li*, Ying Peng, and Jilin Wei, School of Applied Science, Taiyuan University of Science and Technology, Taiyuan 030024, China*

Gao Wang, State Key Laboratory for Electronic Test Technology, North University of China, Taiyuan 030051, China*

Received: 6 January 2018/**Accepted:** 28 April 2018

Abstract. Fire poses a significant risk to the safety, health, and property of people around the world. However, traditional "point sensor" fire detection techniques for indoor buildings based on air particles, air temperatures, and smoke have a low sensitivity, long response time, and poor stability. Therefore, video-based fire detection has become a particularly efficient and important method for detecting the early signs of a fire. Due to image blur, low illumination, flame-like interference and other factors, there is a certain error rate of fire recognition using video flame recognition methods. According to our previous study of a multi-feature flame recognition algorithm, a novel flame recognition algorithm based on free radical emission spectroscopy during combustion is investigated in this paper. First, multiple features are extracted from the video images by employing our proposed processing scheme. Then, the features are post-processed by a temporal smoothing algorithm to eliminate the error recognition rate, which is caused by the similar characteristics of objects between flame-like and real flame areas. In the temporal smoothing experiments, the proposed method achieves the true positive rates of 0.965 and 0.937 for butane flames and forest fire, respectively. Additionally, the spectral signals of OH, CH, C_2 and other free radicals in the combustion objects were acquired by the spectrometer. The vibrational temperature and rotational temperature are calculated after identification of the $A^2\Delta \rightarrow X^2\Pi$ transition of the CH (410–440 nm). The flames-like are completely rejected by the proposed method in the validation experiment. In the subsequent butane combustion experiment, the vibrational temperature of the butane was 4896 K, and the rotational temperature was 2290 K. The experimental results show that real fires can be precisely recognized and that the combustion temperature can be determined from the CH emission spectroscopy. This novel method provides a new viewpoint for fire detection and recognition.

Keywords: Flame recognition, Temporal smoothing, CH free radicals, Emission spectroscopy, Combustion temperature

* Correspondence should be addressed to: Xuanbing Qiu, E-mail: qiuxb@tyust.edu.cn; Chuanliang Li, E-mail: clli@tyust.edu.cn; Gao Wang, E-mail: wanggao@nuc.edu.cn

1. Introduction

Fire is one of the most devastating threats to human life. Rapid and accurate recognition and early warning of fires are the most important ways to minimize casualties and property damage, especially in indoor buildings. Due to the variety of fire initiators, the environmental complexity and the randomness of fire occurrence, it is very difficult to detect and predict fire [1]. At present, fire early warning systems are mainly based on multi-sensor networks [2] and surveillance video image recognition [3–6]. The light produced by the combustion of a flame travels much faster than smoke or heat. On the other hand, the multi-sensor network systems, which include sensors such as smoke sensors, carbon monoxide sensors, temperature sensors and other various kinds of gas sensors, for fire combustion have the disadvantages of low sensitivity, long response time and short detection range [7]. Therefore, fire detection techniques based on computer vision have become increasingly more significant and effective for early fire detection.

With the fast development of image sensor technology, image processing algorithms and computer technology, fire detection techniques based on machine vision or artificial intelligence are viable alternatives for or complements to existing fire detection techniques and have been shown to be useful to solve several problems related to the use of traditional sensors [8, 9]. Increasingly more pattern recognition fire algorithms have emerged, such as the Bayesian classifier [3], artificial neural network [4] and Markov model [5]. Truong et al. [6] proposed a support vector machine multi-feature fire identification method for open spaces; this method has a lower error rate and higher reliability, but its learning is time-consuming. Wang et al. [10] employed the Wald-Wolfwitz stochastic test algorithm to identify real flame and flame-like areas. This adaptive algorithm mainly uses the random fluctuation of flames to identify the fire, but the recognition accuracy is barely satisfactory. Bosch et al. [11] proposed a fire identification method based on the spatial and temporal characteristics of infrared video, which distinguishes between flames and flames-like by detecting the signal strength of thermal objects (heat source). Horng et al. [12] proposed a fire identification method based on HSI (Hue, Saturation, Intensity) color space, which has a short response time. However, because color is only one of the static characteristics of flames, the recognition rate of this method is not extremely satisfactory.

In our previous study, a multi-feature fire recognition algorithm combined with a logarithmic regression method was proposed to realize the rapid identification of fire [13]. First, the image was segmented according to the chromatic characteristics of the flame, and the flame candidate region is obtained by the difference between the moving target and the reference image. Second, multiple features, such as color characteristics, motion characteristics, area rate of change, roundness, numbers of sharp angles, centroid displacement and other characteristics, are extracted to establishment of logarithmic regression model to determine whether there is a fire.

Flame recognition based on image processing has been widely used in fire detection. However, due to various disadvantageous factors such as image blur, low illumination, and flame-like interference, there will always be some error rate. For these situations, fire identification results need to be further post-processed and optimized. As flame-like interferences are generally short-term in images in the video surveillance range, they can be removed by using a temporal smoothing algorithm. In the flame combustion field, the temperature field is a very crucial feature, which can describe the combusting stage and dynamic characteristics of the fire. Therefore, this feature could be selected as a key feature for explaining the combustion stage of the fire and for serving as the scientific basis for fire recognition due to the free radicals produced by the combustion procedure.

When fire occurs, the combustion procedure will produce a large number of free radicals such as OH, CH, C_2 and other intermediates. These free radicals reflect the target temperature field distribution. They can be acquired by using emission spectroscopy [14]. Researchers worldwide have launched a series of studies of flame temperature measurement. Wang et al. [15] used a USB4000 fiber optic spectrometer manufactured by Ocean Optics, Inc., combined with a Levenberg–Marquardt optimization algorithm, to measure the radiation spectroscopy of flames in the wavelength range of visible light and obtained the change in flame temperature and monochromatic emittance. Zhai et al. [16] investigated the molecular structural characteristics inherent in OH radicals and analyzed and calculated the important parameters such as spectral line transition frequency, energy level distribution and Einstein spontaneous emission transition probability of OH radical emission spectroscopy. The experimental results and a comparison of the theoretical calculation spectrum and the experimental spectral data show that the temperature at the root and the center of the flame are 3125 K and 3380 K, respectively. Cao et al. [17] used a laser-induced fluorescence technique to irradiate the free OH radicals of the flame with a laser beam with an absorption wavelength of 308 nm to excite resonance transition. The total fluorescence intensity of the spontaneous emission is proportional to the OH radical concentration in the initial state, and the OH radical concentration was measured.

Therefore, on the basis of our previous study of multi-feature flame identification [13], a flame recognition algorithm based on temperature measurements of FRES during combustion is proposed in this paper. In Sect. 1, the image after the multi-feature fast flame identification is processed by a temporal smoothing operation in order to eliminate the error rate caused by the similar characteristics of the objects in the flame-like and the fire flame areas. Second, the free radical spectroscopy signals of flames from 300 nm to 450 nm bands are acquired in the monitoring region by using a spectrometer. The CH radical spectroscopy features (from 410 nm to 440 nm) are analyzed. Finally, the vibrational temperature and the rotational temperature were calculated to precisely remove the flame-like areas.

2. Experimental Setup

Experimental setup diagram and photo are shown in Fig. 1a, b. First, the CMOS camera with 300 thousand pixels is fixed to capture the image within the monitoring area. Multiple features, such as image color characteristics, motion characteristics, area rate of change, roundness, numbers of sharp angles, centroid displacement and other characteristics, are extracted to construct a logarithmic regression framework for recognizing fire. Meanwhile, the fiber probe will acquire the flame emission spectroscopy, which is transmitted to the spectrometer slit by using free light coupling. Finally, a laptop records real-time emission spectroscopy signals from the inner CCD of spectrometer. The spectroscopy background noise is removed to obtain the flame spectral intensity distribution by using a spectral intensity response coefficient correction. By comparing with the calculated spectra, the rotational temperature and the vibrational temperature of the CH radical in the flame can be obtained. The fire can be monitored not only by the image processing but also by the temperature of the radicals during combustion.

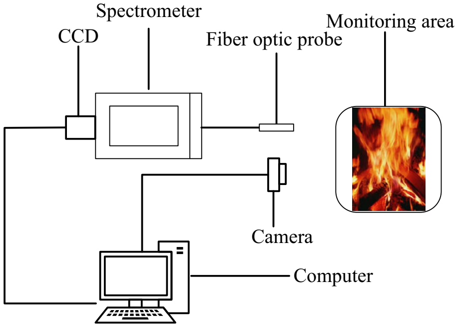

(a)

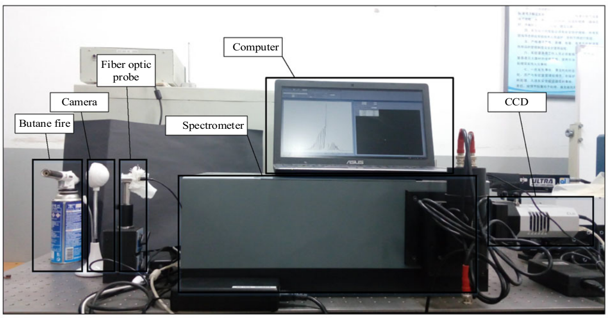

(b)

Figure 1. Experimental setup diagram and photo of fire detection system. (a) The hybrid experimental setup diagram, and (b) the real photo of fire detection system.

The Andor SR-500i spectrometer has a focus length of 500 mm. The aperture is f/6.5, and the spectral resolution is 0.05 nm. After a series of tests, the optimized parameters of the spectrometer were chosen: the blazed grating is 500 nm, exposure time is 0.5 s, and scanning number is 10 times.

3. Fire Recognition Algorithm based on Image Processing

3.1. Multiple Features and the Recognition Algorithm [13, 18]

First, the color feature and motion feature in the video stream are used to determine the candidate flame region (CFR). The average value (m_b, m_r) and the standard deviation (s_b, s_r) of the C_b and C_r components in the YCbCr color space, the area rate of change, the roundness, the numbers of sharp angles, and the centroid displacement were obtained from the candidate flame area. These features are related to whether the video captures a fire.

Second, the multiple features of the images and logarithmic regression recognition algorithm are constructed as follows:

These eight features of the i-*th* frame image can be represented by the linear relationship

$$x = (x_1, x_2, x_3, \ldots, x_8)^T. \tag{1}$$

If the output of the recognition algorithm is binarized, *1* indicates a real flame, *0* indexes a flame-like, and the probability distribution of fire occurrence is subject to a certain probability distribution. Therefore, the probability density function follows the Bernoulli distribution:

$$f(y_i) = p_i^{y_i}(1 - p_i)^{1-y_i} \tag{2}$$

Then, for the *i*-th frame of the video, the output $y_i = 1$ signifies a real flame, and the probability is p_i, while the output $y_i = 0$ signifies a flame-like, and the corresponding probability is $1 - p_i$.

To derive the relationship between the input and the output, it is assumed that the logarithm of fire occurrence probability for the i-*th* frame is a linear combination for each feature:

$$\ln p(\mathbf{x}_i) = a_1 x_{1i} + a_2 x_{2i} + a_3 x_{3i} + \cdots + a_8 x_{8i} = \mathbf{x}_\mathrm{i}^\mathrm{T} \alpha \tag{3}$$

where the coefficient vector is

$$\alpha = (a_1, a_2, a_3, \ldots, a_8)^T. \tag{4}$$

Thus, the flame probability of the i-*th* frame can be denoted as:

$$p_i = \frac{1}{1 + e^{-x_i T \alpha}}. \tag{5}$$

The maximum likelihood estimation method can be used to determine the unknown parameter α:

$$\overset{\wedge}{\alpha}_{MLE} = \arg_{\alpha}\min\prod_{i=1}^{n}\left(\frac{1}{1+e^{-x_i T\alpha}}\right)^{y_i}\left(1-\frac{1}{1+e^{-x_i T\alpha}}\right)^{1-y_i}. \tag{6}$$

To avoid over-fitting of the logarithmic regression, training images are randomly selected. During the training process, the numbers of real and flame-like samples are the same to ensure that the training results are balanced. The maximum likelihood estimation method is used to obtain the coefficient vector, and the probability of the recognition result is calculated according to Eq. (5). Finally, the recognition result is calculated according to the criterion of the suspected CFR:

$$CFR_i = \begin{cases} fire, & if \quad p_i \geq 0.5 \\ non-fire, & if \quad p_i < 0.5 \end{cases}. \tag{7}$$

3.2. Temporal Smoothing Algorithm

If the flame-like objects and real flames have similar characteristics, there will be a recognition error when using traditional recognition approaches [18]. A logarithmic regression has a high sensitivity and false positive rate. The average $\bar{p}_i$ for the probability $\hat{p}_i$ of the past K fire flames can be written as

$$\bar{p}_i = \frac{1}{n}\sum_{k=i-K+1}^{i}\hat{p}_k. \tag{8}$$

Therefore, the error rate and sensitivity of fire detection can be slightly reduced. Figure 2 shows the effect of temporal smoothing in fire detection. For the selected video clip, the actual area of fire flames is represented by the green dash dotted line, *0* for flames-like, and *1* for fire flames. The fire probability without temporal smoothing is shown by the black dashed line. The threshold for fire flame probability is set to 0.5 [18]. Due to noise disturbance, for the real flames and flames-like from 11 s to 13 s and 24 s to 27 s, false alarms occurred by using the raw data. However, the recognition result with temporal smoothing (red solid line) shows that the flame-like areas can be correctly identified for the same video clips. The proposed method can accurately detect the fire flames in the video at 1.2 s, 18.8 s, and 33.8 s, with a 1.6 s delay from visualizing the actual fire flames.

3.3. Experimental Results of Image Processing

In this subsection, 150 real flames and 150 flames-like are used to establish and train the proposed logarithmic regression model. Using the aforementioned chosen criterion, 300 images are randomly selected to avoid over-fitting. A total of 600 butane flame pictures and 255 forest fire pictures are used as true fire examples for

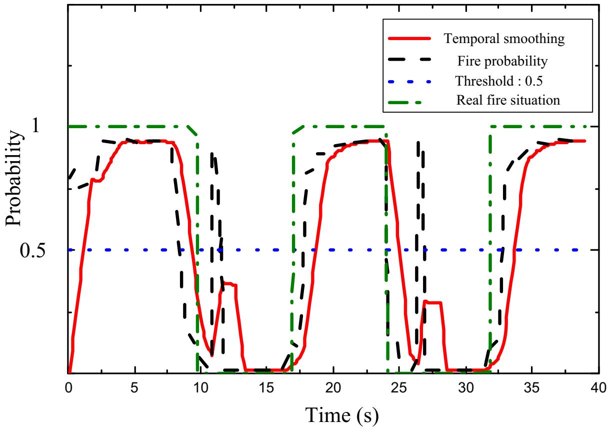

Figure 2. Fire detection experimental results using temporal smoothing algorithm based-video post-processing with the probability threshold of 0.5.

validating our proposed method. A total of 150 red car lights and 6571 images of red clothes were added into our experiment as flames-like to test the negative recognition rate. The recognition rate of the algorithm can be expressed by the TPR (true positive rate) and the TNR (true negative rate). The experimental results are given in Table 1. It can be seen that the TPR is 0.965 and 0.937 for butane flames and forest fires, respectively. Additionally, the TNR is 0.987 and 0.996 for car lights and red clothes, respectively. It can be concluded that the proposed temporal smoothing algorithm is superior to our previous flame recognition approach [10]. These results demonstrate that our method can meet the requirements of flame identification.

4. Emission Spectroscopy of Free Radicals

4.1. Burning State

A series of drastic oxidation reactions are produced between combustion substances and oxygen, accompanied with light and heat emission. This event is called a flame or fire. In the combustion process, there are momentum, heat and mass transmissions among the fuel, oxygen and combustion products. Therefore, those physical and chemical reactions will form a flame. The flame is a complex structure of two-phase flows between high gradients of concentration and temperature. Free radicals are atoms or groups of unpaired electrons that form due to broken covalent bonds in combustible molecules under the interaction of light and heat. Consequently, some free radicals such as OH, CH and C_2 are produced in the combustion process. The temperature, combustion efficiency, and combustion products of the combustion process can be calculated by using emission spectroscopy of the free radicals.

Table 1
Experimental Results Based on Temporal Smoothing Post-processing with Different Video Clips Including Butane Fire, Forest Fire, Car Lights and Red Clothes

Video clips	Butane fire	Forest fire	Car lights	Red clothes
Total fire frames	600	255	0	0
Total fire-like frames	0	0	150	6571
True positive frames	579	239	0	0
False negative frames	21	16	0	0
False positive frames	0	0	2	26
True negative frames	0	0	148	6545
TPR = TP/(TP + FN)	0.965	0.937	–	–
TNR = TN/(FP + TN)	–	–	0.987	0.996

The process of flame combustion is divided into three stages, which can manifest different temperature distributions. During the initial stage, the fire combustion scope is small, and the temperature is low. However, the fire rapidly evolved to the second development stage, where the temperature increases up to 1300 K. During the extinguishing stage, the combustion process is still violent, and the temperature remains high [19]. Therefore, it can be inferred that the temperature distribution is the most significant feature for determination of the fire combustion stage.

4.2. Temperature Measurement Principle of FRES

In the combustion process, the high-speed collision among particles will not only excite the translational degrees of freedom of the particles but also excite the rotation, vibrational and electronic degrees of freedom. At the same time, due to the short time that the particles have the high energy level, the emission spectroscopy of the corresponding frequency is generated when the particles jump from the high energy level to the low energy level. The transition between different energy levels is unique for a specific emission spectrum of each particle. Therefore, particles can be discerned by identifying the emission spectroscopy of a free radical. In addition, each degree of temperature can be derived from the population condition between the energy levels of particles. This is the theoretical basis for emission spectroscopy of a molecule.

The intensity distribution of the FRES is determined by both the structure of the free radical and the respective degrees of temperature; the intensity distribution of the emission spectroscopy is dependent on the respective degree of temperature for the selected free radical. Therefore, the molecular rotational, vibrational and electron temperatures can be derived theoretically by analyzing the intensity distribution of the FRES. The spectrum can be calculated by comparing the theoretical and experimental spectra data to determine the temperature of the respective degrees of freedom.

The spectral intensity $I_{v''N''}^{v'N'}$ of the FRES is defined as the energy emitted by the radiation source per second. It is donated as

$$I_{v''N''}^{v'N'} = N_{v'N'} A_{v''N''}^{v'N'} hc v_{v''N''}^{v'N'} \tag{9}$$

where h is the Planck constant, c is the speed of light, $N_{v'N'}$ is the number of high-energy-level particles, $A_{v''N''}^{v'N'}$ is the Einstein spontaneous emission transition probability, and $v_{v''N''}^{v'N'}$ is the transition frequency. The number of high-energy particles $N_{v'N'}$ is a function of the molecule degrees of freedom,

$$N_{v'N'} = \frac{N_0 g_e}{Q_e Q_v Q_r} \exp\left(-\frac{E_e}{kT_e}\right) \cdot \exp\left(-\frac{E_v}{kT_v}\right) \times (2N' + 1) \cdot \exp\left(-\frac{E_r}{kT_r}\right) \tag{10}$$

where N_0 is the total number of molecules; k is the Boltzmann constant; T_e, T_v and T_r are the electronic temperature, vibrational temperature and rotational temperature, respectively; E_e, E_v and E_r are electronic state, vibration state and the dynamic state of the energy, respectively; g_e is the electronic state degeneracy; N' is the high energy level for the number of revolutions; and Q_e, Q_v and Q_r are the electronic state, vibration state and rotation of the partition function, respectively. It can be seen from the formula that the line intensity $I_{v''N''}^{v'N'}$ is a function of the electron temperature, vibrational temperature, and rotational temperature for the selected molecule.

The line intensities of different rotational and vibrational temperatures can be obtained by using LIFBASE software [20]. Figure 3 shows the spectroscopy results of the rotational temperature of 3000 K and the vibrational temperature from 1000 K to 5000 K. Figure 4 shows the line intensities of the vibrational temperature of 3000 K and the rotational temperature from 1000 K to 5000 K. It is seen from Figs. 3 and 4 that the line intensities characterize different rotational temperatures and vibrational temperatures. As a result, the flame can be recognized and detected by using the line intensities of the emission spectroscopy results.

4.3. Calibration of Combustion Flame Spectra of Butane in the Atmosphere

In this experiment, butane is completely burned and remains stable. If the butane is completely burned, the reaction formula is expressed as

$$2C_4H_{10} + 13O_2 = 8CO_2 + 10H_2O. \tag{11}$$

Some radicals such as OH, CH, and C_2 will form during the combustion process.

The emission spectroscopy signals from 200 nm to 900 nm are depicted in Fig. 5. The longitudinal coordinate indicates the relative line intensity of the emission spectroscopy result for all radicals in the combustion process, and the maximum intensity is defined as a digital number of 1000. As seen in Fig. 5, there are many molecule spectroscopy bands whose emission intensities are much stronger than the background signals in the range of 300 nm to 800 nm. The significant

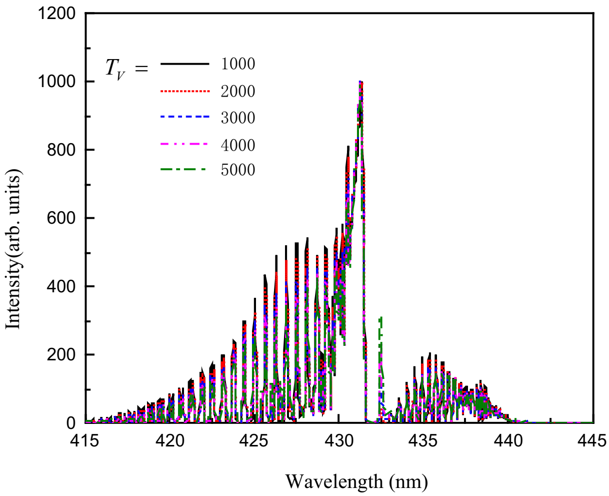

Figure 3. Spectral intensities of different vibrational temperatures from 1000 K to 5000 K by the theoretic calculation of LIFBASE and the experiment.

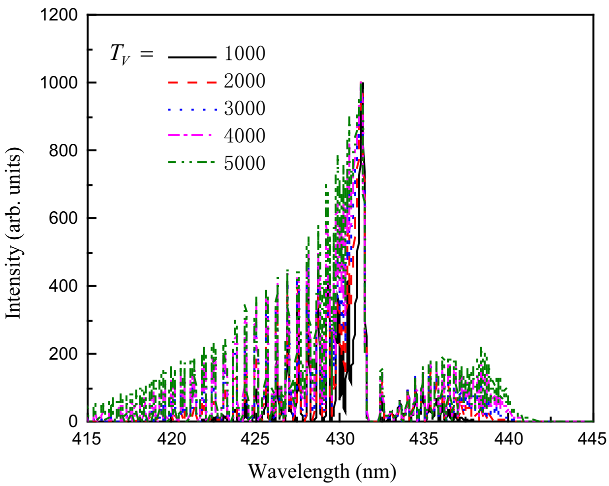

Figure 4. Spectral intensities of different rotational temperatures from 1000 K to 5000 K by the theoretic calculation of LIFBASE and the experiment.

transition spectroscopies include OH $A^2\Sigma^+ \rightarrow X^2\Pi_r$ (300–330 nm), CH $B^2\Sigma^- \rightarrow X^2\Pi$ (380–410 nm), $A^2\Delta \rightarrow X^2\Pi$ (410–440 nm), and C_2 (450–570 nm). In addition, the spectral lines for an atom of Na at 589.0 nm and 589.6 nm and for an atom of C at 766.3 nm and 769.6 nm are evidently found in the emission spectroscopy analysis. It is also seen that the radicals of CH $A^2\Delta \rightarrow X^2\Pi$ (410–

440 nm) have higher strengths and are more favorable for the analysis of their respective temperatures. The radicals and atoms generated in the combustion of butane may characterize the profiles of the flame and be extracted as flame features for the recognition and detection of flame and fire, especially for use in early fire detection.

4.4. Temperature Measurements of CH Spectroscopy

The intensity distributions of the experimental spectra and theoretic calculated spectra are shown in Fig. 6. In Fig. 6, the black solid line and the red dotted line signify the calculated spectrum by LIFBASE and the spectrum obtained by the experiment, respectively.

A Chi square test is used to demonstrate the effectiveness and flexibility of our temperature measurements. A Chi square test is a statistical hypothesis test wherein the sampling distribution of the test statistic is a Chi squared distribution when the null hypothesis is true. It is used to determine whether there is a significant difference between the expected frequencies and the observed frequencies in one or more categories. From Fig. 6, it can be seen that the value of a Chi square test of two spectra signals will reach a minimum if the vibrational temperature increases up to 4896 K and the rotational temperature is 2290 K [21]. Therefore, it can be determined that the vibrational temperature of a CH radical is 4896 K and that the rotational temperature is 2290 K. We measured the spectral signals of the butane fire 8 times and calculated the mean value. Figures 7 and 8 show the measurement errors for the vibrational temperature and rotational temperature. The errors fluctuate from 1.663% to 1.152% and from 1.437% to 1.045% for the vibrational temperature and rotational temperature, respectively. The true

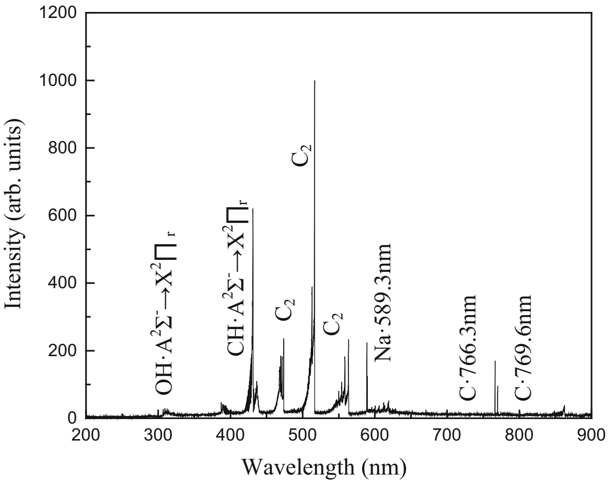

Figure 5. Emission spectral signals for flame of the butane combustion with the wavelength band from 200 nm to 900 nm.

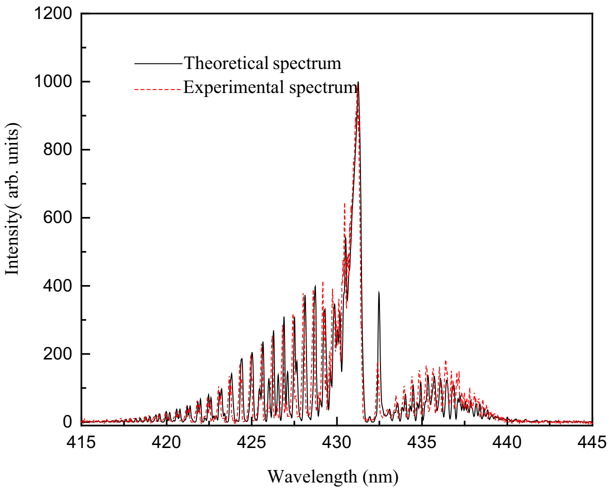

Figure 6. Comparison results of spectral intensities of the theoretical calculated spectrum and experimental obtained spectrum.

energy of the flame can be approximated by the rotational temperature of the free radical, so the temperature of the butane fire is approximately equal to 2296 K. The temperature of the CH free radicals can characterize the temperature of the butane flame. Consequently, early fire detection can be conducted by using the emission temperature from the emission spectroscopy of radicals generated during the combustion of butane.

4.5. Discussion and Declaration

The vibrational and rotational temperatures have been acquired by the foregoing method of CH spectroscopy with the help of the off-line spectrometer in our laboratory. Therefore, the status of fire combustion is inferred, and a fire alarm system can be adopted using the temporal smoothing to denoise the fluctuation extracted from fire videos. However, there are some key problems that should be addressed before this method can satisfy the field demands in practical application.

I. The spectrometer must be a low-cost, portable and compact measurement device for realistic application. The system cost must be similar to a traditional video detection system.
II. The size of the fire alarm system must be as compact as possible and suitable for embedding into the Building Automation System.
III. Our computation time must satisfy the real-time on-line demands.

The low-cost and compact spectrometer Aurora4000 (manufactured by Changchun New Industries Optoelectronics Technology Co., Ltd.) could be qualified for practical application. The fire detection firmware will be programmed using VC++ and OpenCV structure. Above all, this elaborate and essential prepara-

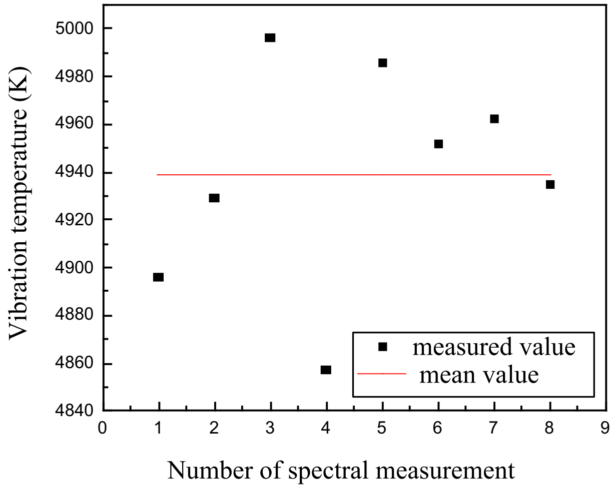

Figure 7. The measurement errors of the vibrational temperatures with the average of 8 times.

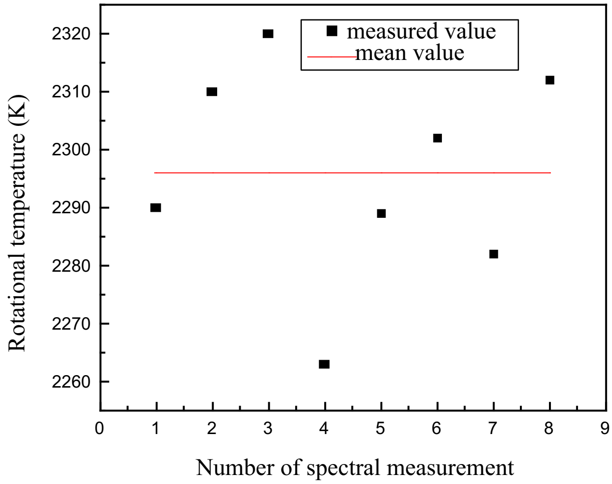

Figure 8. The measurement errors of the rotational temperatures with the average of 8 times.

tion should be performed before our proposed fire detection algorithm is carried out.

5. Conclusion and Future Work

In this paper, a novel hybrid fire detection algorithm is constructed by combining image processing and emission spectral analysis. The temporal smoothing post-processing provides an effective and powerful tool for an improved fire recognition rate. Based on the molecule spectroscopy theory, the relationship between the emission intensity distribution and the rotational and vibrational temperatures of the CH free radical (410–440 nm) electron band is analyzed and investigated. We can infer the flame temperature and make a rough judgment on the burning state of the fire in the field to quickly determine an effective method to put out a potential fire.

The early fire features, especially the emission spectrum, are effective for fire detection, in comparison with other detection methods such as video recordings of smoke and flames and other temperature sensors. As aforementioned, we must carefully address the cost and space demands of real applications. Therefore, the next step in our research will be to develop an integrated, compact, and economic fire detection system based on our proposed method and return to the field to detect fires in field trials.

Acknowledgements

This work was partly supported by the National Natural Science Foundation of China (No. U1610117, 11504256, 61573323), Doctoral Scientific Research Foundation of Taiyuan University of Science and Technology (No. 20132011), the Scientific and Technological Innovation Programs of Higher Education Institutions in Shanxi(No. 2015166), National Undergraduate Training Program for Innovation and Entrepreneurship (No. 2017261 and 2018338).

References

1. Zhang HJ, Zhang N, Xiao NF (2015) Fire detection and identification method based on visual attention mechanism. Optik 126:5011–5018
2. Aslan YE, Korpeoglu I, Ulusoy Ö (2012) A framework for use of wireless sensor networks in forest fire detection and monitoring. Comput Environ Urban Syst 36:614–625
3. Ko BC, Cheong KH, Nam JY (2010) Early fire detection algorithm based on irregular patterns of flames and hierarchical Bayesian Networks. Fire Saf J 45:262–270
4. Wang Y, Yu C, Tu R, Zhang Y (2011) Fire detection model in Tibet based on grey-fuzzy neural network algorithm. Expert Syst Appl 38:9580–9586
5. Wang L, Ye M, Zhu Y (2010) A hybrid fire detection using Hidden Markov Model and luminance map. In A hybrid fire detection using Hidden Markov Model and luminance map, pp 905–915

6. Truong TX, Kim JM (2012) Fire flame detection in video sequences using multi-stage pattern recognition techniques. Eng Appl Artif Intell 25:1365–1372
7. Qureshi WS, Ekpanyapong M, Dailey MN, Rinsurongkawong S, Malenichev A, Krasotkina O (2016) QuickBlaze: early fire detection using a combined video processing approach. Fire Technol 52:1293–1317
8. Prema CE, Vinsley SS, Suresh S (2018) Efficient flame detection based on static and dynamic texture analysis in forest fire detection. Fire Technol 54:1–34
9. Jia Y, Yuan J, Wang J, Fang J, Zhang Q, Zhang Y (2016) A saliency-based method for early smoke detection in video sequences. Fire Technol 52:1271–1292
10. Wang DC, Cui X, Park E, Jin C, Kim H (2013) Adaptive flame detection using randomness testing and robust features. Fire Saf J 55:116–125
11. Bosch I, Gomez S, Molina R, Miralles R (2009) Object discrimination by infrared image processing. In Object discrimination by infrared image processing, pp 30–40
12. Horng WB, Peng JW (2008) A fast image-based fire flame detection method using color analysis. Tamkang J Sci Eng 11:273–285
13. Tingyu X, Xuanbing Q, Dongyuan S, Ning L, Chuanliang L, Gao W, Yu Y (2017) Fast fire flame recognition algorithm based on multi-feature logarithmic regression. J Comput Appl 37:1989–1993
14. Liu YF, Zhang LS, He WL, Huang Y, Du YJ, Lan LJ, Ding YJ, Peng ZM (2015) Spectroscopic study on the laser-induced breakdown flame plasma. Acta Physica Sinica 64:45202
15. Yong-qing W, Yan-ru C, Qi Z, Fei-nan C, Jing-jing C (2012) Multi-spectral measurement of basic oxygen furnace flame temperature. Spectrosc Spectr Anal 32:2920–2924
16. Zhai X, Ding Y, Peng Z, Chen L, Luo R (2012) Temperature determination of an oxy-acetylene flame based on the OH radical emission spectrum. J Tsinghua Univ 52:980–983
17. Liying C, Renming P, Xinggui Q, Yan L, Shengyou L, Mignsheng Y, Qiang X, Fei G, Li W (2010) Method for online measurement of concentration of OH free radical in flame zone of Class B fire and flame device. In Method for online measurement of concentration of OH free radical in flame zone of Class B fire and flame device. China
18. Kong SG, Jin D, Li S, Kim H (2016) Fast fire flame detection in surveillance video using logistic regression and temporal smoothing. Fire Saf J 79:37–43
19. Wenxi D (1985) Analysis and treatment of building structures (1)—fire temperature determination method. Ind Build 15:48–53
20. Luque J (1999) Database and spectral simulation program (Version 1.5), Sri International Report Mp
21. Peng ZM (2011) Measurements of rotational and vibrational temperatures based on flame emission spectroscopy. Acta Physica Sinica 60:104702